

Bursting induced by excitatory synaptic coupling in nonidentical conditional relaxation oscillators or square-wave bursters

Jonathan E. Rubin*

*Department of Mathematics and Center for the Neural Basis of Cognition, University of Pittsburgh,
Pittsburgh, Pennsylvania 15260, USA*

(Received 19 April 2006; revised manuscript received 31 May 2006; published 21 August 2006)

This work explains a mechanism through which the introduction of excitatory synaptic coupling between two model cells, one of which is excitable and the other of which is tonically active when uncoupled, leads to bursting in the resulting two-cell network. This phenomenon can arise when the individual cells are conditional relaxation oscillators, in that they can be tuned to engage in relaxation oscillations, or when they are conditional square-wave bursters. The mechanism is illustrated with a model for conditional pacemaker neurons in the pre-Bötzinger complex as well as with a reduced form of this model. In the relaxation oscillator case, a periodic bursting solution is proved to exist in the singular limit, under a pair of general conditions. These conditions relate the durations of the silent and active phases of the bursting solution to the locations of certain structures in the phase plane, at appropriate synaptic input strengths. Further, additional conditions on the relative flow rates in the silent and active phases are proved to imply the uniqueness and asymptotic stability of the bursting solution.

DOI: [10.1103/PhysRevE.74.021917](https://doi.org/10.1103/PhysRevE.74.021917)

PACS number(s): 87.19.La, 05.45.Xt

I. INTRODUCTION

A wide range of physical systems engage in oscillatory behaviors, switching repeatedly between silent and active phases. Models featuring such silent and active phases are often classified as excitable, corresponding to the existence of a stable critical point in the silent phase, or oscillatory, corresponding to the existence of an unstable critical point about which solutions oscillate. A third possibility is that an attractor can exist in the active phase. This attractor can be a stable critical point, or it can itself be a limit cycle that does not feature an excursion through the silent phase. In models of the behavior of neuronal membrane potential, for example, the silent phase corresponds to relatively hyperpolarized membrane voltages typically associated with a rest state, while the active phase corresponds to significantly depolarized voltages. In this paper, I consider a pair of cells such that when they are uncoupled, one is excitable and the other features an attractor in the active phase. I demonstrate and analyze a mechanism by which coupling the two cells reciprocally with synaptic excitation yields the emergence of periodic bursting behavior in both cells.

This work is motivated by experiments and modeling of the pre-Bötzinger complex (pre-BötC). This region of the mammalian brainstem has been shown to generate rhythmic bursting, which may play a pacemaking role in the inspiratory phase of the respiratory rhythm and in gasping [1]. A subset of cells within the pre-BötC are referred to as conditional pacemakers, in that they are able to engage in rhythmic bursting when parameters, such as applied current or extracellular potassium concentration, are adjusted appropriately. Due to extensive heterogeneities in the network, however, only a subset of these cells show bursting when uncoupled, while others remain silent or engage in tonic

spiking [2,3,1]. A natural question that arises is, how does a network of synaptically coupled pre-BötC cells produce robust, rhythmic bursting in the face of such heterogeneities? Further, how important is the presence of intrinsically bursting cells in inducing bursting in the pre-BötC network? Indeed, building on earlier ideas that an “emergent network-based mechanism,” “group pacemaker,” or “hybrid pacemaker-network” may underlie respiratory oscillations [4–8], a variety of recent experimental results have shown that some aspect of the respiratory rhythm persists under manipulation of burst-supporting pacemaker currents in the pre-BötC [9–12].

Some exploration of these issues has been undertaken in previous modeling work. Butera and colleagues developed a pre-BötC cell model, with a square-wave or fold-homoclinic bursting mechanism [13,14] based on a persistent sodium current [15,16], which compares well with experimentally observed features of pre-BötC bursting [17]. Simulations demonstrate that heterogeneities enhance the range of tonic input levels over which a network of model pre-BötC cells bursts, as well as the frequency range over which bursting can occur. Rybak *et al.* have refined the model and have used simulations to study the contributions of various currents, including heterogeneities in these currents, to pre-BötC activity patterns [18]. Rubin and Terman mathematically analyzed synchronization of a heterogeneous population of model pre-BötC cells, some of which burst and some of which were excitable when uncoupled, in a reduced model featuring persistent sodium current but without standard sodium and potassium spike-generating currents [19]. Further, Best *et al.* used a bifurcation analysis harnessing singular perturbation theory to show how synaptic coupling itself can directly expand the parameter range over which bursting is observed, in a pair of identical full model pre-BötC cells [20].

Here, I again consider a pair of model pre-BötC cells; however, I return to the issue of heterogeneity. In particular,

*Electronic address: rubin@math.pitt.edu

I extend the work of Rubin and Terman by explaining how bursting can emerge when, without coupling, one cell is excitable and the other is tonically active. As in previous modeling work, I consider the synaptic coupling between the cells to be excitatory, based on the experimental finding that pre-BötC bursting persists in a qualitatively similar fashion under blockade of synaptic inhibition [21,3]. The mechanism for coupling-induced bursting relies on two effects of synaptic excitation. First, synaptic excitation from the tonic cell recruits the excitable cell to become active. More surprisingly, the onset and subsequent withdrawal of synaptic excitation from the recruited excitable cell to the tonic cell can cause the tonic cell to fall silent. The latter component can be viewed as a complement to the phenomenon of post-inhibitory rebound, through which synaptic inhibition can activate otherwise silent cells (see, e.g., Refs. [22–24]). I show that these effects can combine to yield bursting under a pair of conditions, which relate the times spent in the silent and active phases of a bursting solution to the locations of certain structures in the phase plane of each cell, at appropriate synaptic input strengths. Further, two additional compression conditions [25] on relative rates of change in certain parts of the silent and active phases are shown to imply the uniqueness and asymptotic stability of the bursting solution.

The mechanism presented here for the existence of synchronized bursting induced by mutual synaptic excitation in conditional relaxation oscillators is similar to one considered previously by Rowat and Selverston [26]. Rowat and Selverston also studied a pair of model cells, each governed by the system

$$\begin{aligned} \tau_m dV/dt &= -[V + q + f(V_{\text{pre}})(V - E_{\text{post}}) - i_{\text{inj}}], \\ \tau_s dq/dt &= -q + \sigma_s(V - E_s), \end{aligned} \quad (1)$$

where $\tau_m < \tau_s$, E_{post} , i_{inj} , and σ_s are constants, with $V < E_{\text{post}}$, where V_{pre} denotes the voltage of the other cell, and where $f(V) = \{1 + \exp[-\gamma(V - \theta)]\}^{-1}$ for parameters γ and θ . The cells are identical in the absence of coupling, and heterogeneity is introduced by assigning each cell a different value of θ . Note that system (1) has linear nullclines in the (V, q) plane and that both cells are at the same rest state, at the intersection of these nullclines (state R in Fig. 1), in the absence of coupling. These features represent simplifications relative to the conditional relaxation oscillator situation considered here, in which one nullcline is cubic and the cells are at different fixed points in the absence of coupling. With coupling, system (1) can give rise to oscillations if the synaptic threshold θ is tuned to be significantly different across the two cells, as shown in Fig.1. The oscillations arise if coupling is introduced when both cells are near R ; however, unlike the relaxation oscillator case, the oscillatory solution coexists with a stable fixed point, as described in the figure caption. The tuning of thresholds in Ref. [26] implies that one cell sends synaptic signals even when it is at rest in the silent phase, while the other fails to do so when at a fixed point, generated by synaptic input, in the active phase, a decoupling of synaptic transmission and activity state that may be less biologically realistic than the relaxation oscillator mechanism considered in the present paper. Moreover,

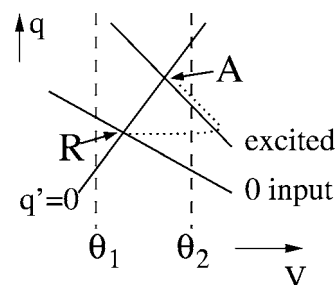


FIG. 1. Nullclines for model (1). Two V -nullclines are shown, one for $i_{\text{syn}}=0$ (labeled 0 input) and one for $i_{\text{syn}}=V-E_{\text{post}}$ (labeled excited). The synaptic thresholds are $\theta = \theta_i$, $i=1,2$. Thus, with coupling, there is a stable fixed point with cell 1 at rest at R , where it sends excitation to cell 2, and cell 2 at rest at A , where it does not send excitation to cell 1. On the other hand, if both cells are placed at R , then the excitation from cell 1 pulls V_2 above θ_2 , as shown by the dotted curve, which initiates oscillations (see Ref. [26]).

the analysis presented here goes beyond the work in Ref. [26] in that conditions are rigorously established under which bursting will emerge in a general class of models, uniqueness and stability of the bursting solution are considered, and the phenomenon is extended to a model system of more than two dimensions.

Previous authors have also considered emergent bursting in heterogeneous cellular populations [27] and in particular have shown that a silent cell and a tonically active cell can engage in rhythmic bursting when coupled diffusively [28–30]. The mechanism that produces bursting in the presence of diffusive coupling, however, is quite different from that which arises under synaptic coupling. In the diffusive case, in the absence of coupling, the cells are not capable of bursting. The introduction of coupling induces bistability in the fast subsystem for the coupled cell network, and under appropriate conditions, bursting results. Heterogeneity is not required for this effect but does enhance it. The synaptic excitation that I consider has no qualitative effect on the fast subsystem bifurcation structure, and the coupling-induced mechanism presented in this paper depends fundamentally on the presence of heterogeneity.

Section II of the paper focuses on the case of conditional relaxation oscillators and consists of four subsections. In the first, the relevant model equations, and structural hypotheses on these equations, are introduced. Following this, the bursting mechanism is explained, using nullclines generated from the pre-BötC model for illustrative purposes. While this work is motivated by issues arising from past work on the pre-BötC, it is quite general, and Sec. II C presents the analytical proof that certain conditions are sufficient for periodic bursting to arise, as well as for uniqueness and asymptotic stability of the periodic bursting solution, when synaptic excitation is introduced between any two model cells satisfying certain general hypotheses, in the singular limit. Extensions of these conditions are presented in Sec. II D. In Sec. III, I explain the bursting mechanism in conditional square-wave bursting model cells. The presentation makes use of bifurcation diagrams for a fast subsystem but does not include a fully detailed mathematical treatment. Finally, the paper concludes with a discussion section and an appendix containing

some details about the particular pre-BötC models used in simulations.

II. RELAXATION OSCILLATORS

A. Model equations

Consider, for $i \in \{e, t\}$, a system of ordinary differential equations of the form

$$v_i' = f_i(v_i, h_i) + g_{\text{syn}} s_j (v_{\text{syn}} - v_i) \equiv F_i(v_i, h_i, s_j), \quad j \neq i,$$

$$h_i' = \epsilon g_i(v_i, h_i),$$

$$s_i' = \alpha s_{\infty}(v_i)(1 - s_i) - \beta s_i, \quad (2)$$

where $0 < \epsilon \ll 1$, $\alpha, \beta > 0$, and $s_{\infty}(v)$ is a monotone increasing function taking values in $[0, 1]$. For notational convenience, let

$$s_{\infty}(v) = 1 / \{1 + \exp[-(v - \theta_s) / \sigma_s]\}, \quad \sigma_s > 0, \quad (3)$$

with a limiting case of $s_{\infty}(v) = H(v)$, the Heaviside step function, as $\sigma_s \downarrow 0$; however, the results here carry over to more general forms of $s_{\infty}(v)$. In the neuronal case, each $v_i(t)$ represents the membrane potential of a cell (with capacitance scaled to 1), each h_i is an associated channel state variable, and each s_i modulates the strength of the synaptic coupling current from cell i to cell j . Note that $g_{\text{syn}} s_j > 0$, such that as long as $v_{\text{syn}} > v_i$, the coupling term gives a positive contribution to v_i' . Coupling for which $v_{\text{syn}} > v_i$ over most relevant values of v_i is called excitatory. Also note that the interval $I_s := [0, \alpha / (\alpha + \beta)]$ is positively invariant for s , and let

$$s_{\text{max}} := \frac{\alpha}{\alpha + \beta}.$$

The following assumptions will be made on system (2); also see Fig. 2.

(A) For $i \in \{e, t\}$ and fixed $s_j \in I_s$, the v -nullcline, $\{(v_i, h_i) : F_i(v_i, h_i, s_j) = 0\}$, defines a cubic-shaped curve, composed of left, middle, and right branches, in the (v_i, h_i) phase plane, with $F_i > 0$ ($F_i < 0$) above (below) this curve.

Denote the branches of $F_i = 0$ by $v = v_L^i(h, s)$, $v = v_M^i(h, s)$, $v = v_R^i(h, s)$, with $v_L^i < v_M^i < v_R^i$ for each (h, s) on which all three functions are defined.

(B) For $i \in \{e, t\}$, the h -nullcline, $\{(v_i, h_i) : g_i(v_i, h_i) = 0\}$, is a monotone decreasing curve in the (v_i, h_i) plane, with $g_i > 0$ ($g_i < 0$) below (above) this curve. For fixed $s_j \in I_s$, the h -nullcline intersects $F_i = 0$ at a unique point $p_i(s_j) = (v_{\text{FP}}^i(s_j), h_{\text{FP}}^i(s_j))$.

(C) For $i = e$, $p_e(0)$ lies on the left branch of $\{(v_e, h_e) : v_e = v_L^e(h_e, 0)\}$. For $i = t$, for all $s \in I_s$, $p_t(s)$ lies on $\{(v_t, h_t) : v_t = v_R^t(h_t, s)\}$.

(D) The line $\{v = \theta_s\}$, for θ_s appearing in Eq. (3), intersects the curve $\{v = v_M^i(h, s)\}$ for both possible i and for all $s \in I_s$.

Remark 2.1: The results of this paper carry over directly if (A)–(C) are modified such that the h -nullcline is monotone increasing and the cubic v -nullcline has its left knee at lower h than its right knee, as in FitzHugh-Nagumo, Morris-Lecar, and various other models.

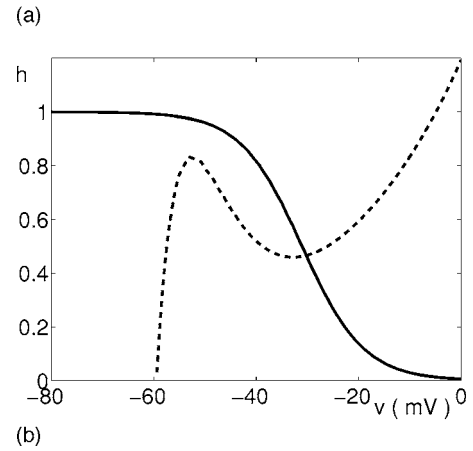
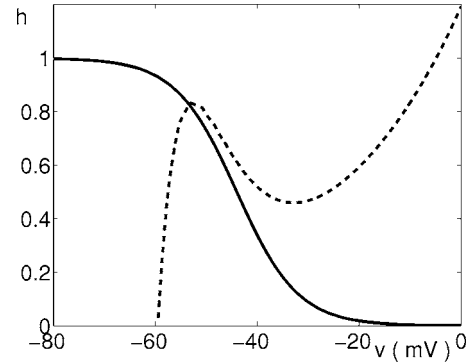


FIG. 2. Top: Nullclines for an excitable, or silent, cell. The v -nullcline is dashed, while the h -nullcline is solid. In this and all other nullcline figures, the x axis corresponds to v in mV, while the y axis corresponds to the dimensionless variable h . Bottom: Nullclines for a tonically active, or spiking, cell.

In a neuron, a bursting solution alternates repeatedly between silent phases of relatively constant, low voltage and active phases featuring voltage spikes, which are rapid voltage oscillations of significant amplitude. A model of the form (2) can be obtained from a model bursting neuron by omitting some spike-generating currents but maintaining a current that allows for transitions to an elevated voltage state. In this model, a bursting solution consists of an oscillation composed of silent phases, with $v_i \approx v_L^i(h, s)$, alternating with active phases, with $v_i \approx v_R^i(h, s)$. Assumptions (A)–(C) justify the notation $i \in \{e, t\}$: when uncoupled, the cell labeled by $i = e$ has a stable critical point in the silent phase and hence is excitable, while the cell labeled by $i = t$ has a stable critical point in the active phase, corresponding to a sustained active, or tonic, state, for all coupling strengths.

Remark 2.2: In fact, the v -nullcline need not be triple-branched for the tonic cell for s large, as long as the cell still has a stable critical point for such s . Thus, (A) can in fact be weakened, as long as (C) is adjusted to ensure that the critical point exists.

Assumptions (A)–(B) hold in particular for the reduced form of the pre-BötC cell model from Ref. [15] that is considered in Ref. [19], which will be used to illustrate the general results in this section. For a single cell within a network, this model takes the form

$$C_m v' = I_{\text{NaP}} + I_L + I_{\text{syn}} + I_{\text{app}},$$

$$\begin{aligned}
 h' &= [h_\infty(v) - h]/\tau_h(v), \\
 s' &= \alpha_s(1-s)s_\infty(v) - s/\tau_s,
 \end{aligned}
 \tag{4}$$

where $I_{\text{NaP}} = -g_{\text{Na}}m_\infty(v)h(v - E_{\text{Na}})$, $I_L = -g_L(v - E_L)$ and where h_∞, m_∞ are monotonic decreasing and increasing sigmoidal functions, respectively. The first equation in (4) describes the evolution of the voltage across a cell's membrane, with capacitance C_m , in terms of a persistent sodium current (I_{NaP}), a leak current (I_L), and synaptic (I_{syn}) and applied (I_{app}) input currents. The function I_{syn} takes the form $I_{\text{syn}} = g_{\text{syn}}s_{\text{tot}}(E_{\text{syn}} - v)$, where $s_{\text{tot}} \geq 0$ encodes the activity level of the cells giving inputs to this one, and the current I_{app} is simply assumed to be constant. The second equation in (4) describes the slow inactivation of the persistent sodium current. For biophysically relevant parameter values, (4) can be considered as singularly perturbed, since h evolves much more slowly than v . Finally, $s_\infty(v)$ is given in (3). The full functional forms and parameter values used in system (4) are given in the Appendix.

B. Illustration of the emergent bursting mechanism

I now illustrate how synaptic coupling can allow bursting to emerge for a system of the form (2) under hypotheses (A)–(D), using two coupled cells of the form (4) as an example. Rigorous results concerning general features that are sufficient for the existence, uniqueness, and asymptotic stability of this emergent bursting solution will follow this illustration, in Sec. II C.

Figure 2 shows nullclines for two copies of system (4), with the nullcline $h = h_\infty(v)$ of the variable h shifted so that one copy has a stable critical point on the left branch of its dashed v -nullcline and the other copy has a stable critical point on the right branch of its v -nullcline, as specified in (C). In the notation of system (2), we have $f_e = f_i$ but $g_e \neq g_i$.

In the absence of synaptic coupling, the two cells rest at their respective stable critical points. Suppose that synaptic coupling is introduced as in system (2), with each cell receiving input from the other but not from itself. Then the two cells can indeed engage in sustained, periodic bursting oscillations, as shown for system (4) in Fig. 3. Here, the oscillations were initiated by giving the excitable cell initial conditions $(v_e, h_e) = (-20, 0.8)$. In the absence of synaptic coupling, the cell would have made a single excursion and then returned to the critical point on the left branch of its v -nullcline.

To understand the mechanism for the bursting, note that although system (2) consists of six equations, we can decompose these into three equations for each cell. Moreover, we can project each (v_i, h_i, s_i) into the (v_i, h_i) phase plane, keeping in mind that the location of the v_i -nullcline depends on the level of the synaptic variable s_j , which is in turn determined by (v_j, h_j) . For example, Fig. 4 shows the same nullclines seen in Fig. 2, plus an additional, shifted v -nullcline (also dashed) for each cell, corresponding to the maximal level of synaptic input that each cell receives during the bursting oscillations shown in Fig. 3. Although it is

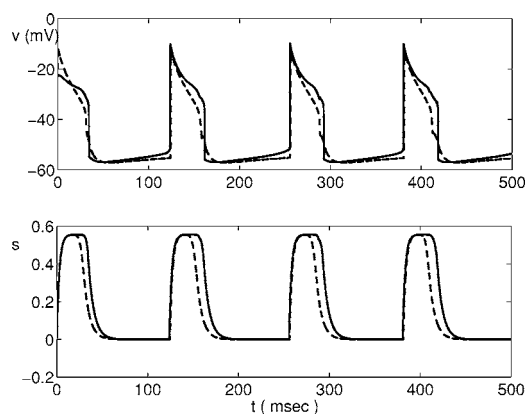


FIG. 3. Sustained bursting oscillations in the presence of strong synaptic coupling. The top panel shows voltage traces versus time, while the bottom shows synaptic conductances versus time. The solid curves correspond to the cell that is tonically active in the absence of coupling, while the dashed correspond to the cell that is silent in the absence of coupling.

somewhat difficult to discern, the shifted v -nullclines are in fact cubic functions of v , with shallow negatively sloped middle branches near $v = -40$. Figure 4 also shows thick black curves, corresponding to the start of the bursting oscillations shown in Fig. 3. From the trajectory in the bottom panel, we see that because the excitable cell in the top panel enters the active phase, the tonic cell receives synaptic input from it and thus moves to its lowered v -nullcline. Note that for visibility in Fig. 4, the tonic cell was started at $(v_t, h_t) = (-23, 0.55)$, slightly away from its fixed point $p_t(0) = (v_{FP}^t(0), h_{FP}^t(0))$, but simulations verify that the same solution results if the cell starts at $p_t(0)$.

In fact, in the example shown in Fig. 4, the cell that on its own is tonically active would remain tonically active if this synaptic input were sustained; that is, it still has a stable critical point $p_t(s_{\text{max}})$ at elevated v on its lowered v -nullcline. Note, however, that this lowered critical point occurs at a lower level of h , corresponding to greater inactivation of I_{NaP} , than $h_{FP}^t(0)$. The previously silent cell, which does not have a critical point in the active phase, eventually falls down to the silent phase (i.e., the left branch of its v -nullcline); see Fig. 5. This allows the synaptic input to the tonic cell to decay. But because the availability of its I_{NaP} has been reduced, it can no longer stay active, and instead it falls into the silent phase, as shown in Fig. 5. In terms of nullclines, the key point is that the lowered critical point for the tonic cell lies below the right knee of its unexcited, or 0 input, v -nullcline, such that synaptic decay on the fast time scale causes it to fall down to the silent phase.

Once both cells are in the silent phase, as synaptic excitation decays, the formerly silent, excitable cell approaches the stable critical point $p_e(0)$, but the formerly tonic cell has no such point. Thus, the tonic cell is eventually able to jump up to the active phase and resume spiking again. The portions of the trajectories of the pre-BötC cells corresponding to this phase of the emergent bursting solution are also shown in Fig. 5.

Finally, when the tonic cell resumes spiking, it synaptically excites the silent cell, pulling it up to the active phase,

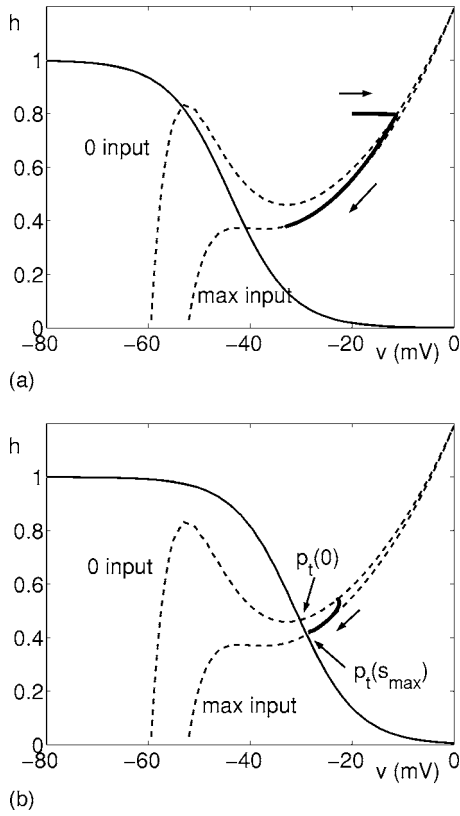


FIG. 4. Original and excited nullclines for both cells. Each h -nullcline is a thin solid curve and all v -nullclines are dashed. Original nullclines are labeled as *0 input*, while the excited nullclines correspond to maximal synaptic input and are thus labeled as *max input*. The thick black curves correspond to the first 26 ms of the oscillations shown in Fig. 3. The arrows alongside these curves show the direction of flow. The variable h (y axis) decreases along each trajectory; that is, the trajectories evolve downward in the panels shown as time increases. Top: resting cell. Bottom: tonically active cell, with critical points $p_t(0)$ and $p_t(s_{\max})$ labeled.

as shown in Fig. 6. This completes one burst cycle. Note that in the sustained bursting oscillations, the formerly tonic cell leads entry into the active phase, while the formerly silent cell leads the return to the silent phase, although this is not apparent on the scale used in Fig. 3.

C. General conditions for emergent bursting

In this section, conditions are established under which a periodic bursting solution can be constructed for system (2), under (A)–(D), in the singular limit of $\epsilon \downarrow 0$. Results on geometric singular perturbation theory suggest that this construction will yield the existence of a nearby bursting solution for $\epsilon > 0$ sufficiently small [31], although checking the details may be technically involved.

To begin the analysis, let us call the points in (v, h) space where any two branches of a cubic-shaped v -nullcline meet the *knees* of this nullcline. Specifically, under (A), for fixed $s \in I_s$, the left branch $(v_L(h, s), h)$ meets the middle branch $(v_M(h, s), h)$ in the left knee of the v -nullcline, while the

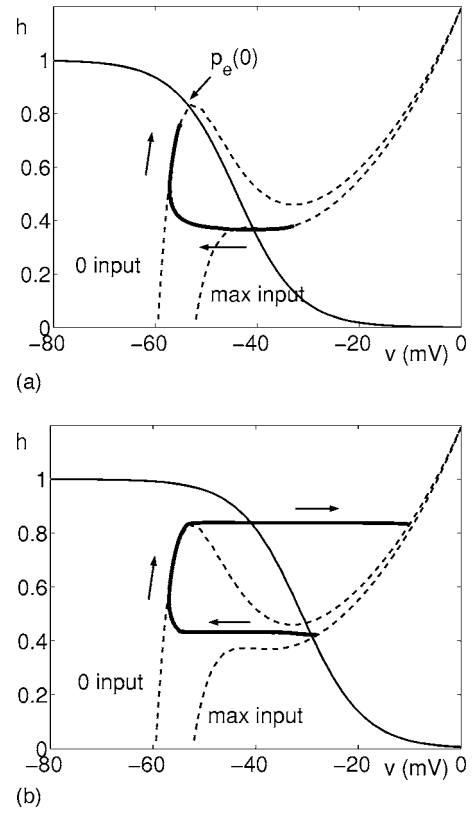


FIG. 5. Continuation of trajectories from Fig. 4. The entry of the excitable cell (top panel) into the silent phase allows decay of synaptic excitation to the tonic cell (bottom panel), which also enters the silent phase. In the silent phase, the excitable cell approaches the stable critical point $p_e(0)$, but the tonic cell eventually jumps back to the active phase again.

middle branch meets the right branch $(v_R(h, s), h)$ in the right knee. For each $s \in I_s$, let $(v_{LK}^i(s), h_{LK}^i(s))$ denote the left knee of the v -nullcline for cell i and, similarly, let $(v_{RK}^i(s), h_{RK}^i(s))$ denote the right knee of the v -nullcline for cell i .

For system (2), there are associated fast and slow subsystems. The fast subsystem is obtained by setting $\epsilon = 0$ directly and thus takes the form

$$v_i' = F_i(v_i, h_i, s_j), \quad j \neq i,$$

$$h_i' = 0,$$

$$s_i' = \alpha s_\infty(v_i)(1 - s_i) - \beta s_i. \quad (5)$$

Recall that $i \in \{e, t\}$, so this is a system of six equations.

To define slow subsystems, set $\tau = \epsilon t$ and let the overdot denote differentiation with respect to τ . Under this rescaling of time, system (2) becomes, with $i \in \{e, t\}$,

$$\epsilon \dot{v}_i = F_i(v_i, h_i, s_j), \quad j \neq i,$$

$$\dot{h}_i = g_i(v_i, h_i),$$

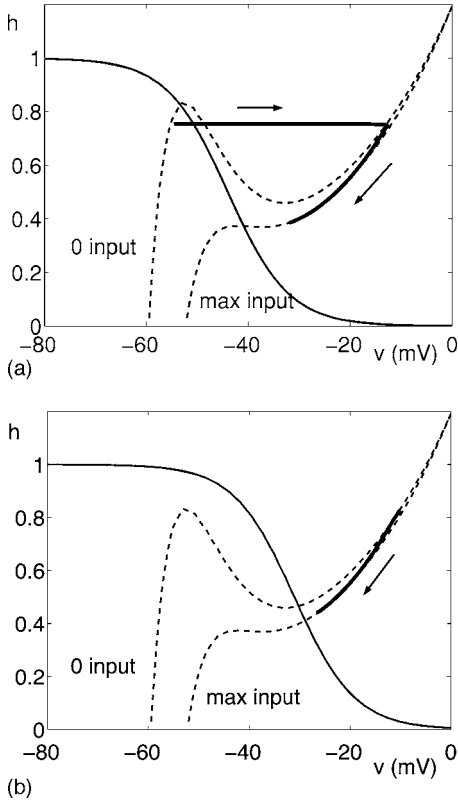


FIG. 6. Completion of one burst cycle, continued from Fig. 5. The trajectories shown extend from the entry of the excitable cell (top panel) into the active phase to a moment shortly before the excitable cell jumps back down to the silent phase.

$$\epsilon \dot{s}_i = \alpha s_{\infty}(v_i)(1 - s_i) - \beta s_i. \quad (6)$$

The slow subsystems are obtained from system (6) by setting $\epsilon=0$, solving the algebraic equations, and inserting the results into the h -equation. This process yields, for each i ,

$$\dot{h}_i = g_i(v_X^i(h_i, s_j), h_i), \quad j \neq i, \quad (7)$$

for $X \in \{L, M, R\}$. Since the branch $v_M(h, s)$ is unstable with respect to the fast subsystem, there are four distinct slow subsystems (7) that could theoretically be relevant, assuming $s_{\infty}(v) = H(v - \theta_s)$. When both cells are silent, the relevant slow subsystem is

$$\dot{h}_e = G_L^e(h_e) := g_e(v_L^e(h_e, 0), h_e), \quad (8)$$

$$\dot{h}_i = G_L^i(h_i) := g_i(v_L^i(h_i, 0), h_i). \quad (9)$$

When both cells are active, the relevant slow subsystem is

$$\dot{h}_e = G_R^e(h_e) := g_e(v_R^e(h_e, s_{\max}), h_e), \quad (10)$$

$$\dot{h}_i = G_R^i(h_i) := g_i(v_R^i(h_i, s_{\max}), h_i). \quad (11)$$

The other two subsystems involve combinations of left-hand and right-hand terms, but this paper will not provide these explicitly as it turns out that they will not be needed here.

A key point is that the singular bursting solution consists of a concatenation of solutions of systems (5), (8) and (9), and (10) and (11). Projected to each (v, h) -plane, the solutions to system (5) consist of jumps between branches of v -nullclines for different values of s , while the solutions to the slow subsystems take the form of pieces of these nullclines.

From consideration of Figs. 4 and 5, it is clear that two general conditions are needed to allow the possibility of bursting. Heuristically, the first condition states that there must be a possibility that synaptic input from the tonic cell can recruit the excitable cell to the active phase, while the second allows the possibility that after both cells are active, the loss of synaptic input from the excitable cell to the tonic cell may cause the tonic cell to fall down to the silent phase. In the notation of Sec. II B and the above paragraph, these conditions read

$$h_{\text{FP}}^e(0) > h_{\text{LK}}^e(s_{\max}); \quad (12)$$

that is, the h coordinate of the fixed point (FP) of the excitable cell without input lies above the h coordinate of the left knee (LK) of the v -nullcline of this cell with maximal input, and

$$h_{\text{FP}}^i(s_{\max}) < h_{\text{RK}}^i(0); \quad (13)$$

that is, the h coordinate of the fixed point of the tonic cell with maximal input lies below the h coordinate of the right knee (RK) of the v -nullcline of this cell without input.

After the details of the construction of a singular bursting solution are presented, conditions (12) and (13) will be refined.

Remark 2.3: Condition (13) typically requires stronger synaptic input than condition (12). This is because it is a condition involving active phase structures. Voltages in the active phase are closer to the reversal potential of synaptic excitation, typically $v_{\text{syn}} \approx 0$ mV, than those in the silent phase. Hence, a larger s is needed to induce changes in these structures, relative to $s=0$, than is needed for silent phase structures. This effect is responsible for the larger difference present between the left knees than between the right knees in Figs. 2 and 4–6.

Next, I present the construction of a periodic singular bursting solution for system (2). To do this, I will take $s_{\infty}(v) = H(v - \theta_s)$, such that $s_{\infty}(v_i) = 0$ ($=1$) when cell i is in the silent (active) phase. There will be two unknowns that play key roles in this construction. These are T_A , which is the time, on the slow time scale, that the cells spend in the active phase, and T_S , the slow time scale time that the cells spend in the silent phase. In the singular limit, as will be shown more explicitly below, the time in the active phase is indeed the same for both cells, so there is no ambiguity in the definition of T_A , and similarly for T_S . The construction will yield conditions under which there exists a unique pair (T_A, T_S) for which a periodic singular bursting solution exists.

Let us start the construction at time $\tau=0$ with both cells in the silent phase, with the tonic cell at the left knee of the relevant v -nullcline. Since the synaptic decay rate, denoted β in system (2), is $O(1)$ with respect to ϵ , $s_e=s_i=0$. Hence, the left knee of the v -nullcline for the tonic cell is in fact $(v_{LK}^i(0), h_{LK}^i(0))$. As time starts to evolve from this initial arrangement, the tonic cell immediately jumps up to the active phase, and $s_i \rightarrow s_{max}$ on the fast time scale. To get things started, assume that the excitable cell is above the left knee $(v_{LK}^e(s_{max}), h_{LK}^e(s_{max}))$. Condition (12) ensures that this is possible, but we will need to check later that this emerges from the complete construction. From such a position, the onset of synaptic excitation causes the excitable cell to jump immediately to the active phase as well. The first piece of the singular solution for each cell consists of its jump up to the active phase, under the flow of the fast subsystem (5).

By (B)–(C), the tonic cell has a stable critical point in the active phase for $s=s_{max}$, while the excitable cell does not. Thus, the ensuing active phase continues, with $s=s_{max}$, until the excitable cell reaches the right knee of its v -nullcline. Denote the time from the jump up to the active phase until this knee is reached by T_A . Note that at time T_A , the return of the excitable cell to the silent phase implies that $s_e \rightarrow 0$ on the fast time scale.

Where is the tonic cell at time T_A ? Because the excitable jumps immediately to the active phase when the tonic cell does, the tonic cell enters the active phase with $(v_i(\tau=0), h_i(\tau=0)) = (v_R^i(h_{LK}^i(s_{max}), s_{max}), h_{LK}^i(s_{max}))$. So its position $(v_i(T_A), h_i(T_A))$ is determined by evolving the h_i equation of the slow subsystem (10) and (11), from this initial condition, for time T_A . By condition (13), the resulting position may be below the right knee $(v_{RK}^i(s=0), h_{RK}^i(s=0))$, in which case the tonic cell returns to the silent phase at time T_A as well. Assume for now that this is indeed the case. The second and third pieces of the singular solution for each cell come from the evolution of the slow subsystem (10) and (11) for time T_A and the jump down to the silent phase under the fast flow of (5), respectively.

By (C), the excitable cell approaches the equilibrium point $p_e(0)$ in the silent phase. Hence, the duration of the silent phase is determined by the time it takes for the tonic cell to evolve from $(v_i(T_A), h_i(T_A))$ to the left knee $(v_{LK}^i(0), h_{LK}^i(0))$, where it was at the start of the construction. Call this time T_S . The final piece of the singular bursting solution consists of the slow subsystem trajectories in the silent phase generated by system (8) and (9). After time T_S , the tonic cell jumps back up to the active phase, while the excitable cell jumps up if and only if it lies above the left knee $(v_{LK}^e(s_{max}), h_{LK}^e(s_{max}))$.

From the above construction, it is clear that T_S is a function of T_A . Similarly, if we prescribe a fixed T_S , then there is a unique corresponding T_A . This is found by evolving the initial condition $(v_{RK}^e(s_{max}), h_{RK}^e(s_{max}))$ under Eq. (8) in the silent phase for time T_S , and then computing the time it takes to evolve from the resulting position back to $(v_{RK}^e(s_{max}), h_{RK}^e(s_{max}))$ under Eq. (10) in the active phase.

To characterize the properties of the functions $T_S(T_A)$ and $T_A(T_S)$, it is helpful first to define the following four times; see Fig. 7.

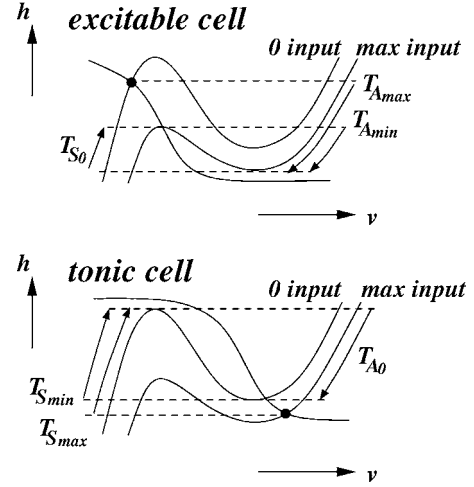


FIG. 7. Nullclines for an excitable cell and a tonic cell, with 0 and maximal input, and associated active and silent phase durations defined in the text.

(i) Let $T_{A_{min}}$ denote the time of evolution from initial condition $(v_R^e(h_{LK}^e(s_{max}), s_{max}), h_{LK}^e(s_{max}))$ to $(v_{RK}^e(s_{max}), h_{RK}^e(s_{max}))$ under Eq. (10).

(ii) Let $T_{A_{max}}$ denote the time of evolution from initial condition $(v_R^e(h_{FP}^e(0), s_{max}), h_{FP}^e(0))$ to $(v_{RK}^e(s_{max}), h_{RK}^e(s_{max}))$ under Eq. (10).

(iii) Let $T_{S_{min}}$ denote the time of evolution from initial condition $(v_L^i(h_{RK}^i(0), 0), h_{RK}^i(0))$ to $(v_{LK}^i(0), h_{LK}^i(0))$ under Eq. (9).

(iv) Let $T_{S_{max}}$ denote the time of evolution from initial condition $(v_L^i(h_{FP}^i(s_{max}), 0), h_{FP}^i(s_{max}))$ to $(v_{LK}^i(0), h_{LK}^i(0))$ under Eq. (9).

Next, a lemma can be proved.

Lemma 2.4: Assume that (A)–(D) and (12) and (13) hold.

(a) The function $T_S(T_A)$ is a monotonic increasing function defined on an interval of the form $[T_{A_0}, \infty)$, with $T_S(T_{A_0}) = T_{S_{min}}$. This function approaches asymptotically to $T_{S_{max}}$ as $T_A \rightarrow \infty$.

(b) The function $T_A(T_S)$ is a monotonic increasing function defined on an interval of the form $[T_{S_0}, \infty)$, with $T_A(T_{S_0}) = T_{A_{min}}$. This function approaches asymptotically to $T_{A_{max}}$ as $T_S \rightarrow \infty$.

Proof: (a) The time T_A is always computed from the flow of (10), with both cells in the active phase. The tonic cell always enters the active phase at $(v_R^i(h_{LK}^i(0), 0), h_{LK}^i(0))$ in the (v_i, h_i) plane, and it evolves with $\dot{h}_i < 0$ there by (B). By (ii), there exists some minimal T_A value after which the tonic cell lies below the right knee $(v_{RK}^i(0), h_{RK}^i(0))$, and for all larger T_A , the tonic cell falls down to the silent phase when $s_e \rightarrow 0$ at time T_A . This minimal T_A value defines T_{A_0} such that $T_{S_{min}} = T_S(T_{A_0})$.

Now, for $T_A > T_{A_0}$, the tonic cell monotonically (in h_i , and hence in v_i) approaches the fixed point $p_i(s_{max}) = (v_{FP}^i(s_{max}), h_{FP}^i(s_{max}))$ in the active phase. Hence, larger T_A values cause the tonic cell to enter the silent phase at lower h_i values. Since the time T_S is always computed from the flow of (9), with $\dot{h}_i > 0$, from the time that both cells enter

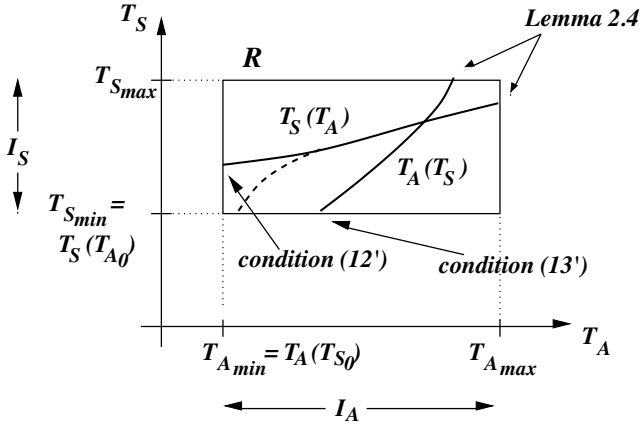


FIG. 8. The curves $T_S(T_A)$ and $T_A(T_S)$ in (T_A, T_S) space, inside the rectangle R . Note that a unique intersection is ensured (see Proposition 2.9) if both curves have positive slope < 1 , as shown here. The results that imply the locations of the intersections of these curves with the sides of R are used to label each intersection. The dashed curve represents an alternative path for $T_S(T_A)$ that still yields an intersection with $T_A(T_S)$, corresponding to the replacement of condition (12') with condition (12'').

the silent phase until the tonic cell reaches $(v_R^t(h_{LK}^t(0), 0), h_{LK}^t(0))$, smaller starting values of h_t yield larger T_S , and the desired monotonicity is established. Finally, the tonic cell approaches arbitrarily close to the fixed point $p_t(s_{max})$ in the active phase as $T_A \rightarrow \infty$, which gives the asymptotic behavior of T_S .

(b) The proof for $T_A(T_S)$ is similar, based on the fact that the excitable cell always enters the silent phase at the same point but flows to different positions depending on the value of T_S . Condition (12) gives the existence of T_{S_0} . \square

Consider the rectangle $R := I_A \times I_S$ in (T_A, T_S) space, where $I_A := [T_{A_{min}}, T_{A_{max}}]$ and $I_S := [T_{S_{min}}, T_{S_{max}}]$. In theory, the curves $T_S(T_A)$ and $T_A(T_S)$ can be used to define an iteration in this space: for fixed $T_A \in I_A$, the next silent phase duration will be $T_S(T_A)$, the subsequent active phase duration will be $T_A[T_S(T_A)]$, and so on. However, this iteration can only be continued as long as each $T_A > T_{A_0}$ and each $T_S > T_{S_0}$. The existence of a periodic singular bursting solution holds if and only if the monotone increasing curves $T_S(T_A)$ and $T_A(T_S)$ intersect inside R , as shown in Fig. 8.

Sufficient conditions under which such an intersection is guaranteed to occur, which are stronger and more precise than (12) and (13), are given in the following theorem.

Theorem 2.5: *Given that (A)–(D) hold for system (2), this system has a periodic singular bursting solution if the following two conditions hold:*

$$T_{A_{min}} > T_{A_0}. \quad (12')$$

$$T_{S_{min}} > T_{S_0}. \quad (13')$$

Remark 2.6: Condition (12') states that if the excitable cell jumps up to the active phase from the minimal possible h_e level, given by the height of the left knee of the excited v_e -nullcline, then the tonic cell will have enough time in the

active phase to get below the right knee of the unexcited v_t -nullcline. Condition (13') is analogous, stipulating that even if the tonic cell jumps down from this right knee, leading to the shortest possible silent phase, the excitable cell will still be able to jump up at the end of the silent phase.

Proof: The implications of conditions (12') and (13') and Lemma 2.4 are illustrated in Fig. 8. First, note that (12') is only possible if (13) holds, while (13') requires (12). Hence, Lemma 2.4 holds under conditions (12') and (13'). Now, we seek an intersection of $T_S(T_A)$ and $T_A(T_S)$ in $R = I_A \times I_S$. Condition (12') ensures that T_S is defined on all of I_A . Since T_S is monotonic increasing with $T_S(T_{A_0}) = T_{S_{min}}$ by Lemma 2.4, condition (12') implies that $T_S(T_{A_{min}}) > T_{S_{min}}$. Moreover, the asymptotic behavior of T_S given in Lemma 2.4 implies that $T_S(T_{A_{max}}) < T_{S_{max}}$. Hence, $T_S(I_A)$ is strictly contained in I_S . Similarly, by condition (13') and Lemma 2.4, $T_A(I_S)$ is well defined and is strictly contained in I_A . These conditions guarantee the existence of the desired intersection. \square

Conditions (12') and (13') are sufficient but certainly not necessary for the existence of a bursting solution. The proof of Theorem 2.5 immediately generalizes to the following.

Corollary 2.7: (12') can be replaced by

$$T_A(T_{S_{min}}) > T_{A_0}, \quad (12'')$$

as long as (13') also holds. Similarly, (13') can be replaced by

$$T_S(T_{A_{min}}) > T_{S_0}, \quad (13'')$$

as long as (12') also holds.

Remark 2.8: Of conditions (12') and (13'), it is (12') that is more likely to fail, by Remark 2.3, since the tonic cell may evolve slowly in the active phase as it approaches the critical point $p_t(s_{max}) = (v_{FP}^t(s_{max}), h_{FP}^t(s_{max}))$, and $h_{RK}^t(0)$ may be very close to $h_{FP}^t(s_{max})$.

It remains to consider the uniqueness of the periodic singular bursting solution, as well as its stability with respect to perturbations in slow variable positions along the nullclines in the silent and active phases. In fact, defining stability in this sense, the following result holds.

Proposition 2.9: *The periodic singular bursting solution of system (2), given by Theorem 2.5, is unique and asymptotically stable if $T_S(T_A)$ and $T_A(T_S)$ are Lipschitz, with Lipschitz constants less than 1, on I_A and I_S , respectively.*

Proof: Suppose that the curves $T_A(T_S)$ and $T_S(T_A)$ intersect in two points, say (T_{A_1}, T_{S_1}) and (T_{A_2}, T_{S_2}) . Let η_A, η_S denote the Lipschitz constants of these curves, with $\eta := \max\{\eta_A, \eta_S\} < 1$. Then

$$\begin{aligned} |T_{S_2} - T_{S_1}| &= |T_S(T_{A_2}) - T_S(T_{A_1})| \leq \eta |T_{A_2} - T_{A_1}| \\ &= \eta |T_A(T_{S_2}) - T_A(T_{S_1})| \leq \eta^2 |T_{S_2} - T_{S_1}|. \end{aligned}$$

Hence, $\eta < 1$ implies $T_{S_2} = T_{S_1}$, which gives $T_{A_2} = T_{A_1}$ as well, by the monotonicity of these curves shown in Lemma 2.4, and thus establishes the uniqueness of the solution.

The stability of the unique solution follows immediately as well, as can be seen, for example, from cobwebbing in (T_A, T_S) space; see Fig. 8. \square

The functions $T_S(T_A), T_A(T_S)$ will be Lipschitz on I_A and I_S , respectively, if the vector field of system (2) is Lipschitz. In fact, there are quite natural compression conditions [25] guaranteeing that $T_S(T_A), T_A(T_S)$ have Lipschitz constants less than one.

For example, consider the impact that an increase in T_A , say from $T_{A_1} \in I_A$ to $T_{A_2} \in I_A$, has on the tonic cell. Denote the tonic cell's position, after time T_{A_1} in the active phase, by $(v_t(T_{A_1}), h_t(T_{A_1}))$, which is uniquely defined since the tonic cell always starts the active phase at $(v_R^t(h_{LK}^t(s_{max}), s_{max}), h_{LK}^t(s_{max}))$. Since $T_{A_1} \in I_A$, $h_t(T_{A_1}) < h_{RK}^t(0)$. Typically, the tonic cell will, at $(v_t(T_{A_1}), h_t(T_{A_1}))$, already lie close to $p_t(s_{max}) = (v_{FP}^t(s_{max}), h_{FP}^t(s_{max}))$ on the v_t -nullcline. During time $(T_{A_1}, T_{A_2}]$, the tonic cell evolves according to Eq. (11). However, if the cell is indeed close to $p_t(s_{max})$, then $|G_R^t(h_t)|$ will be small during this time and little change in h_t will occur,

$$|h_t(T_{A_2}) - h_t(T_{A_1})| \leq \int_{T_{A_1}}^{T_{A_2}} \bar{G}_R^t d\tau,$$

where $\bar{G}_R^t := \max_{h_t \in H_A} |G_R^t(h_t)|$ and $H_A := (h_{RK}^t(0), h_{FP}^t(s_{max}))$.

After the jump down, the tonic cell evolves in the silent phase according to Eq. (9). However, the tonic cell has no fixed point in the silent phase. Hence, the positive quantity $G_L^t(h_t)$ is expected to be larger than $|G_R^t(h_t)|$ for all $h_t \in H_A$. Suppose there exists $\delta > 0$ such that

$$G_L^t(h_t) - |G_R^t(h_t)| > \delta \quad \text{for all } h_t \in H_A. \quad (14)$$

Under this assumption, the time τ^* for the h_t -coordinate of the tonic cell to reach $h_t = h_t(T_{A_1})$, from $h_t = h_t(T_{A_2})$ under Eq. (9), is clearly less than $T_{A_2} - T_{A_1}$.

The time $T_S(T_{A_2})$ is given by $T_S(T_{A_1})$ plus this extra time τ^* and hence

$$T_S(T_{A_2}) - T_S(T_{A_1}) < T_{A_2} - T_{A_1}$$

results. The uniformity of the bound δ in (12) implies that this contraction occurs uniformly on I_A .

Similarly, the excitable cell has a fixed point $p_e(0) = (v_{FP}^e(0), h_{FP}^e(0))$ in the silent phase. Changes in T_S values, say from T_{S_1} to T_{S_2} within I_S , lead to small changes in h_e in the silent phase, since h_e is contracted toward $p_e(0)$ during (T_{S_1}, T_{S_2}) . Given a resulting change in h_e , it will likely take less time than $T_{S_2} - T_{S_1}$ for the excitable cell to cover this distance in the active phase, since it has no fixed point there. This contraction is ensured if there exists $\gamma > 0$ such that

$$|G_R^e(h_e) - G_L^e(h_e)| > \gamma \quad \text{for all } h_e \in (h_{LK}^e(s_{max}), h_{FP}^e(0)). \quad (15)$$

The above arguments, together with Proposition 2.9, establish the following theorem and show that its compression conditions are quite natural, given the fixed point structure assumed in (A)–(C).

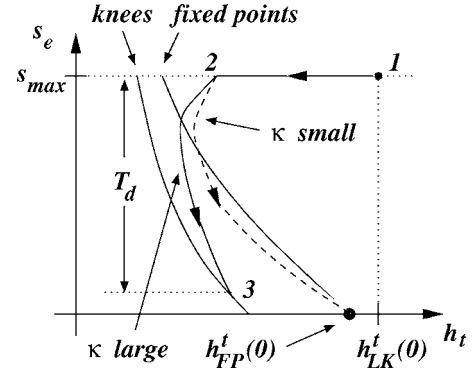


FIG. 9. The phase plane for the tonic cell in the active phase. The curves of knees and fixed points are defined by system (2) with $\beta = \epsilon\kappa$. The tonic cell always enters the active phase at the point labeled 1. Once there, it evolves with $s = s_{max}$ until time T_A , when the excitable cell jumps back to the silent phase. For this illustration, it is supposed that this occurs when the tonic cell is at the point labeled 2. Note that the position of 2 is uniquely determined by T_A . After time T_A , the flow of the tonic cell is governed by system (14). If κ is small, then the tonic cell converges to $(h_{FP}^t(0), 0)$ and the tonic cell remains active. If κ is large, then the tonic cell can jump down to the active phase by hitting the curve of knees, which occurs at the point labeled 3 in the figure. The position of 3 is also uniquely determined by T_A , and therefore the time T_d , defined as the time of flight from point 2 to point 3, is uniquely determined by T_A as well.

Theorem 2.10: Assume that (A)–(D) and (12') and (13') [or (12'') and (13') or (12') and (13'')] are satisfied. The resulting periodic singular bursting solution is unique and asymptotically stable if inequalities (14) and (15) hold.

D. Extensions

The results of Sec. II C can be extended in at least two ways. First, the excitable cell may be allowed to become oscillatory, with its fixed point on the middle branch of the v -nullcline, when $s = s_{max}$. In this case, its h coordinate need not lie above the left knee of its excited v -nullcline, call it $\mathcal{N}_e(s_{max})$, for bursting to occur. If it does not, then when the tonic cell becomes active and $s_t \rightarrow s_{max}$, the excitable cell will jump to the left branch of $\mathcal{N}_e(s_{max})$. It will evolve there until it jumps up from the left knee of $\mathcal{N}_e(s_{max})$. In this scenario, the duration T_A of the active phase will always be given by the time for h_e to evolve, under Eq. (10), from $h_{LK}^e(s_{max})$ down to $h_{RK}^e(s_{max})$. In fact, this time is exactly our $T_{A_{min}}$, and hence there may be an interval of T_S over which $T_A(T_S)$ takes the constant value $T_{A_{min}}$. If $T_S(T_{A_{min}})$ is within this interval, then the bursting solution will feature such a jump to $\mathcal{N}_e(s_{max})$. If not, then the location of the excitable cell's fixed point with $s = s_{max}$ is irrelevant.

A second extension is to allow a slow decay of excitation, taking $\beta = \epsilon\kappa$ in Eq. (2). In this case, once the excitable cell jumps down to the silent phase, the jump down of the tonic cell is no longer ensured. The analysis of this jump down requires consideration of a two-dimensional slow subsystem for the tonic cell, namely

$$\begin{aligned} \dot{h}_t &= g_t(v_R^t(h_t, s_e), h_t), \\ \dot{s}_e &= -\kappa s_e. \end{aligned} \quad (16)$$

Within the (h_t, s_e) phase plane corresponding to the active phase, one can plot a monotone decreasing curve of knees and a monotone decreasing curve of fixed points, defined from the tonic cell components of the full system (2), specifically the v_t -nullclines (parametrized by s_e) and their intersections with the h_t -nullcline; see Fig. 9. The only true fixed point of system (16) lies at $(h_{FP}^t(0), 0)$, however.

As earlier, let $(v_t(T_A), h_t(T_A))$ denote the position of the tonic cell when the excitable cell jumps down. Consider the flow of system (16) from the initial condition $(h_t(T_A), s_{max})$, where it lies when the excitable cell jumps down. Depending on $h_t(T_A)$, if κ is sufficiently large, then the trajectory of (16) will reach the curve of knees and the tonic cell will jump down as well, whereas if κ is too small, the trajectory will converge to $(h_{FP}^t(0), 0)$ and the tonic cell will remain active, both of which are illustrated in Fig. 9.

The delay in the jump down of the tonic cell, after that of the excitable cell, implies that $s_e \neq s_t$ in the silent phase. Denote the duration of this delay, on the slow time scale, by T_d . Since $s = s_{max}$ always holds in the active phase, and the tonic cell always enters the active phase at $(v_t, h_t, s_t) = (v_R^t(h_{LK}^t(0), 0), h_{LK}^t(0), s_{max})$, each T_A on some interval defines a unique T_d . At the same time, T_A uniquely defines the level of h_t when the tonic cell jumps down to the silent phase; see Figs. 9 and 10.

Now, during the delay, s_e reaches $s_{max}e^{-\kappa T_d}$, based on system (16). During the silent phase, say $\tau \in [T_d, T_d + T_S]$,

$$\begin{aligned} s_e &= s_{max}e^{-\kappa\tau}, \\ s_t &= s_{max}e^{-\kappa(\tau - T_d)}. \end{aligned} \quad (17)$$

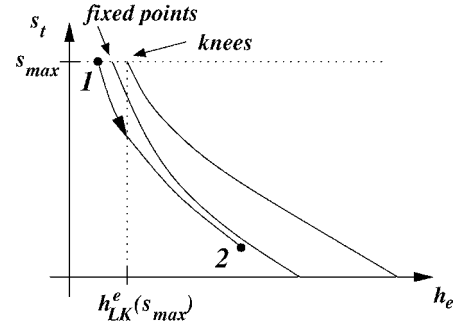
The evolution of both cells in the silent phase is given by the nonautonomous system

$$\begin{aligned} \dot{h}_e &= g_e(v_L^e(h_e, s_t), h_e), \\ \dot{h}_t &= g_t(v_L^t(h_t, s_e), h_t), \end{aligned} \quad (18)$$

with s_t, s_e from Eq. (17). The silent phase ends when the tonic cell reaches a knee $(v_{LK}^t(s_e), h_{LK}^t(s_e))$. Which knee is reached is uniquely determined by the pair $(T_A, T_d(T_A))$, based on the h_t value where the cell enters the silent phase, the evolution of the h_t -equation in system (18) for s_e specified in (17), and the family of v_t -nullclines parametrized by s . Further, for fixed (T_d, T_S) , the value of h_e when the tonic cell jumps up is fixed, and as long as this h_e exceeds $h_{LK}^e(s_{max})$, the excitable cell will jump up as well, yielding a fixed duration T_A of the ensuing active phase duration; see Fig. 10.

In summary, as long as κ is sufficiently large, it is possible to iterate from $T_A^0 \rightarrow (T_d^0, T_S^0) \rightarrow T_A^1 \rightarrow (T_d^1, T_S^1) \rightarrow \dots$, with $T_d^i = T_d(T_A^i)$, $T_S^i = T_S(T_A^i)$, $T_A^{i+1} = T_A(T_d^i, T_S^i)$ for each $i \geq 0$. Conditions (12') and (13') [or (12'') and (13'') or (12') and (13'')] should generalize to conditions for existence, unique-

excitable cell



tonic cell

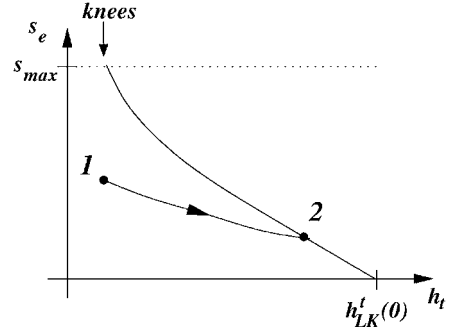


FIG. 10. Phase planes for both cells in the silent phase, including relevant curves of fixed points and knees. The trajectories shown start, at the points labeled *I*, when the tonic cell first enters the silent phase, such that the excitable cell has already been there for time T_d and thus $s_e < s_{max}$. The position of the excitable cell at *I* is exactly that shown at point *3* of Fig. 9 and is determined by T_d ; note that the knees here are left knees, as opposed to right knees in Fig. 9. After time T_S , the tonic cell reaches the curve of knees, with both cells at the points labeled *2*. The location of the tonic cell at *2* is uniquely determined by its initial condition, hence $T_S = T_S(T_A)$. Given the T_d -dependent initial condition for the excitable cell, its position at *2*, and hence the duration of the ensuing active phase, is determined by the T_S imposed by the tonic cell.

ness, and stability of the periodic singular bursting solution in this case. For similar arguments, based on two-dimensional slow flows in singularly perturbed systems arising in other small neuronal networks, see Refs. [23,32,33], for example.

III. CONDITIONAL SQUARE-WAVE BURSTING MODELS

The full pre-BötC model developed by Butera *et al.* [15] can be transitioned from silence to bursting to tonic spiking by varying one of several parameters, and hence the model pre-BötC cells are referred to as conditional bursters. When these cells burst, they engage in square-wave bursting. When a square-wave bursting solution in a model with one slow variable is projected to a two-dimensional space corresponding to one fast variable and the slow variable, it can be seen that the onset of the active phase is generated by the drift of the slow variable past a knee of the curve of equilibrium

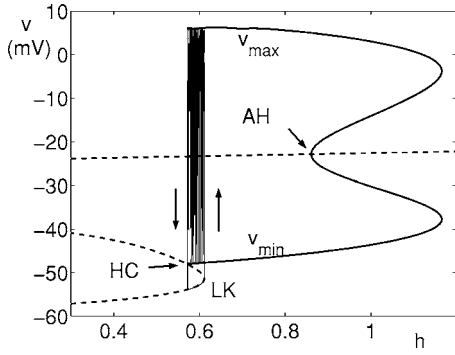


FIG. 11. Square-wave burst solution superimposed on fast subsystem bifurcation structure, generated by an uncoupled model pre-BötC cell, given by system (17) with $g_{\text{syn-e}}=0$ and $g_{\text{tonic-e}}=0.3$. The dashed curve is the projection of the equilibria of the (v, n) equations to the part of the (v, h) plane shown. AH indicates a subcritical Andronov-Hopf bifurcation, which gives rise to a family of unstable periodic orbits. The unstable family ends in a saddle-node bifurcation with a family of stable periodic orbits, along which v varies between v_{max} and v_{min} . This family ends in a homoclinic bifurcation, and HC labels the corresponding homoclinic point. The bursting trajectory drifts along the lower equilibrium branch, with $h' > 0$, until it reaches the knee (LK), jumps up (upward arrow), and begins oscillating. During the oscillations, the solution drifts along the stable periodics, with $h' < 0$ when averaged over each oscillation. Eventually the solution reaches a small neighborhood of the homoclinic orbit and returns to the silent phase (downward arrow).

points of the fast subsystem. During the active phase, the solution travels along a family of periodic orbits. The jump from the active phase to the silent phase occurs when the solution reaches the end of this family, which typically corresponds to a homoclinic bifurcation for the fast subsystem. In the silent phase, the solution drifts along a curve of fast subsystem equilibria, and when the solution reaches the knee of this curve, the burst cycle repeats [13]; see Fig. 11. Alternatively, the model is silent, but excitable, when there is a stable equilibrium point of the full system on the lower branch of the fast subsystem equilibrium curve and is tonically active when there is a periodic orbit of the fast subsystem around which the net drift of the slow variable is zero, yielding a corresponding periodic orbit of the full system. Synaptic inputs can shift the location of the fast subsystem bifurcation structures (e.g., Ref. [20]). In this section, I will explain how coupling two conditional square-wave bursters, one excitable and one tonic, with synaptic excitation can lead to bursting in the two-cell network, through a generalized form of the relaxation oscillator mechanism discussed in the preceding section.

For purposes of illustration, I will focus on the model that motivated this study, namely the full pre-BötC model of Butera and colleagues [15,16]. For a network of two reciprocally coupled cells, with $i \in \{e, t\}$, this model takes the form

$$v_i' = (-I_{\text{NaP}} - I_{\text{Na}} - I_K - I_L - I_{\text{tonic-e}} - I_{\text{syn-e}})/C_m,$$

$$n_i' = [n_\infty(v_i) - n_i]/\tau_n(v_i),$$

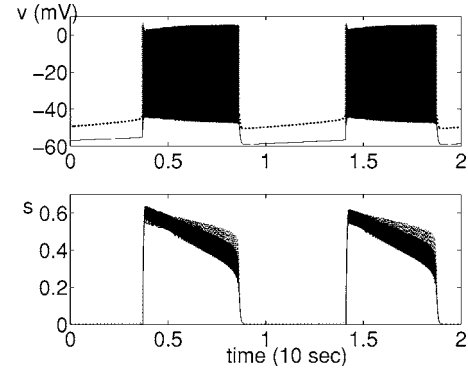


FIG. 12. Emergent bursting oscillation of a formerly tonically active cell (dotted, $g_{\text{tonic-e}}=0.72$ nS) coupled to a formerly excitable cell (solid, $g_{\text{tonic-e}}=0.24$ nS) with $g_{\text{syn-e}}=2$ nS and $\tau_s=50$ ms. Top: voltage. Bottom: synaptic variable. Note that the voltage time courses for the two cells blend together during the active phase, while their synaptic time courses are indistinguishable in the silent phase.

$$h_i' = [h_\infty(v_i) - h_i]/\tau_h(v_i),$$

$$s_i' = \alpha_s(1 - s_i)s_\infty(v_i) - s_i/\tau_s, \quad (19)$$

with intrinsic ionic currents $I_{\text{NaP}} = \bar{g}_{\text{NaP}} m_{P,\infty}(v_i) h_i (v_i - E_{\text{Na}})$, $I_{\text{Na}} = \bar{g}_{\text{Na}} m_\infty^3(v_i) (1 - n_i) (v_i - E_{\text{Na}})$, $I_K = \bar{g}_K n_i^4 (v_i - E_K)$, and $I_L = \bar{g}_L (v_i - E_L)$. Note that $\tau_h(v)$ in system (19) is sufficiently large such that the rate of change of h is significantly slower than the rates of change for the other variables. Thus, h can be used as a bifurcation parameter in the fast (v, n, s) subsystem for a single cell to generate a diagram along the lines of Fig. 11.

In addition to terms for intrinsic currents, the membrane potential equation in system (17) includes a background input current $I_{\text{tonic-e}} = g_{\text{tonic-e}}(v_i - E_{\text{syn-e}})$ and the synaptic coupling current $I_{\text{syn-e}} = g_{\text{syn-e}} s_j (v_i - E_{\text{syn-e}})$ for $j \neq i$. The function $s_\infty(v)$ takes the form (3), and, as in the preceding section, $E_{\text{syn-e}}$ is chosen such that $E_{\text{syn-e}} > v_i$ over the relevant range of v_i values, corresponding to excitatory coupling. Other functional definitions and parameter values for system (19) are listed in the Appendix. Following past work [16,19], I will focus on heterogeneity in the input parameter $g_{\text{tonic-e}}$, but as will be apparent from discussion of the mechanism involved, similar effects can arise through any heterogeneity that causes one cell to be intrinsically silent, makes the other cell intrinsically tonic, and yields certain features when the cells are coupled via synaptic excitation.

Figures 12 and 13 show bursting oscillations (v in the top panel, the synaptic variable s in the bottom panel) for a synaptically coupled pair of cells, given by system (17), with differing $g_{\text{tonic-e}}$ values (given in the captions, along with values for $g_{\text{syn-e}}$ and τ_s). In both cases, one cell was excitable in the absence of coupling, while the other was tonically active. It is already known that in this model, coupling two intrinsically tonic cells by synaptic excitation can cause the pair to burst [16,20]. In the case of Fig. 13, the $g_{\text{tonic-e}}$ value used for the tonic cell is so large that if both cells had this value, they would both be tonically active with the synaptic

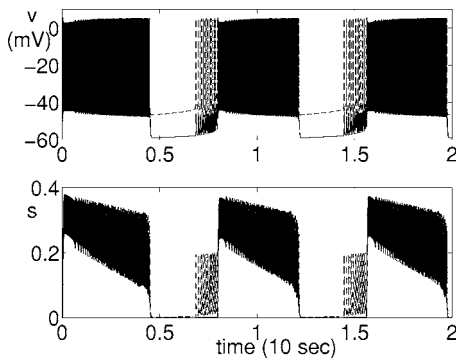


FIG. 13. Emergent bursting oscillation of a formerly tonically active cell (dashed, $g_{\text{tonic-e}}=0.96$ nS) coupled to a formerly excitable cell (solid, $g_{\text{tonic-e}}=0.24$ nS) with $g_{\text{syn-e}}=4$ nS and $\tau_s=50/3$ ms. Top: voltage. Bottom: synaptic variable.

coupling strength used, whereas if both cells had the value used in Fig. 12, then they would burst when coupled with the coupling strength used there.

As in the relaxation oscillator case for $\epsilon \neq 0$, the tonic cell leads the entry into the active phase of the burst (see Fig. 13), while the excitable cell leads the return to the silent phase (i.e., the burst termination). The key to how this works is the impact of synaptic excitation on the bifurcation structures shown in Fig. 11. Figures 14 and 15 show the trajectories from Fig. 13 superimposed on bifurcation diagrams for the formerly excitable cell (Fig. 14) and the formerly tonically active cell (Fig. 15). Figure 14 in particular emphasizes the mechanism for the bursting. In these figures, the S-shaped curves are equilibrium points for the (v, n) subsystem of (19), with h treated as a parameter to be varied and with s fixed. A subcritical Andronov-Hopf bifurcation occurs on the upper branch of each equilibrium curve, giving rise to an unstable family of periodic orbits. Each unstable family terminates in a saddle-node bifurcation with a stable family of periodics, which extends toward lower h values and ter-

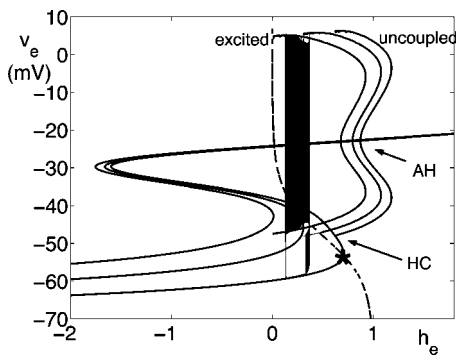


FIG. 14. Bursting oscillation of a formerly excitable cell superimposed on relevant bifurcation structures. Structures corresponding to larger synaptic input levels are farther to the left. The asterisk labels the unique equilibrium point for the $i=e$ equations of system (17) when the cells are uncoupled. AH refers to an Andronov-Hopf bifurcation, while HC refers to a homoclinic point at which the family of periodic orbits born in the AH bifurcation (through a subcritical mechanism) terminates. Both are labeled here for the uncoupled case.

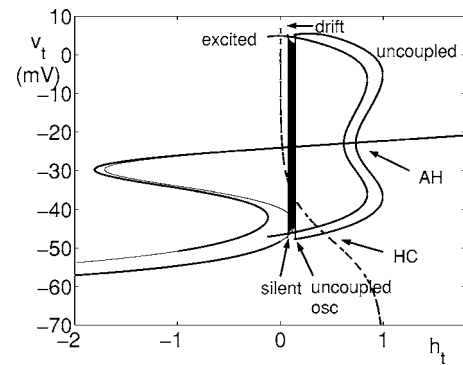


FIG. 15. Bursting oscillation of a formerly tonically active cell superimposed on relevant bifurcation structures. Labels are as in Fig. 14, plus the label drift indicates the direction of drift the cell experiences in the active phase due to synaptic input from the excitable cell, the label silent phase portion of the cell's trajectory lies, and the label uncoupled osc indicates the lower extent in v_t of the tonic spiking solution in the absence of coupling.

minates in a homoclinic bifurcation. Curves in Fig. 14 are shown for different levels of s , namely $s=0$ (uncoupled) and two positive s values, corresponding approximately to the average level of s_t that results over one oscillation when the tonic cell alone is active and the average level of s_t that results over a single fast (active phase) oscillation when both cells are active, near the end of the active phase of a burst. Similarly, in Fig. 15, curves are shown for $s=0$ and for an average level of s_e when both cells are active, near the end of the active phase. Note that synaptic excitation shifts both the equilibrium curve and the family of periodics leftward, to smaller h values. The former shift tends to promote jumps up to the active phase, while the latter promotes the continuation of oscillations at smaller h values within the active phase.

More specifically, in Fig. 14, note the existence of a stable equilibrium point for the $i=e$ equations of system (19) without coupling, marked by the asterisk where the dashed h_e -nullcline intersects the uncoupled (rightmost) fast subsystem equilibrium curve in the silent phase. The excitable cell would rest at this state in the absence of coupling. With coupling, the middle equilibrium curve and family of periodics become relevant. The h_e value at the rest state is above the knee of the middle nullcline, and hence the synaptic input from the tonically active cell pulls the excitable cell up to the active phase, as shown.

When the excitable cell activates, it sends synaptic excitation to the tonic cell, causing the tonic cell to spike at higher voltages and leading to an even greater synaptic input to the excitable cell, such that the leftmost equilibrium curve and family of periodics become relevant. These curves correspond to a relatively high level of excitation to the excitable cell, however. As can be appreciated from Figs. 12 and 13 the input levels that the cells receive actually vary significantly while both cells are active. Thus, even though the trajectory of the excitable cell in Fig. 14 remains to the right of the excited homoclinic orbit, it receives less than this level of input over much of the time it is in the active phase, and

it jumps back to the silent phase when it falls below the homoclinic of some intermediate family of periodics.

Without input, the tonic cell remains in the active phase (uncoupled osc in Fig. 15). From Fig. 15, however, it is apparent that the values of h_t drift lower, to the left of the uncoupled family of periodic orbits (drift in Fig. 15), due to the synaptic coupling from the excitable cell. When the excitable cell returns to the silent phase, the loss of excitation to the tonic cell leaves it below the uncoupled homoclinic orbit, such that as long as the synaptic excitation decays sufficiently fast, the tonic cell returns to the silent phase as well. Finally, after drifting along the lower branch of the equilibrium curve (silent in Fig. 15), the tonic cell is able to exit the silent phase even without coupling, since there is no critical point on this branch, and the cycle repeats.

As in the relaxation oscillator case, certain conditions must be met for bursting to emerge when an excitable cell and a tonically active cell are coupled via synaptic excitation. Indeed, conditions (12) and (13), and their refinements, generalize directly to this higher-dimensional setting in the singular limit, with the homoclinic orbit replacing the right knee in considerations of the jump down to the silent phase. A condition needed for the tonic cell to jump down, analogous to (13), is that the excitable cell must remain active long enough such that the tonic cell travels below the homoclinic orbit for the uncoupled case, as seen in Fig. 15. After it jumps down, the tonic cell must remain silent long enough to enable the excitable cell to follow it into the active phase, which is analogous to (12). In part, this depends on the duration of the previous active phase, since the longer the tonic cell stays active, the lower its h_t value becomes and the longer it subsequently takes to jump up again. Likewise, the duration of the active phase depends on that of the previous silent phase.

A complication relative to the relaxation oscillator case, however, is that the growth and decay rates of s play more subtle roles in the full conditional bursting system. This subtlety arises because s changes on each oscillation, whereas it is effectively constant during the active phase in the relaxation oscillator case. As noted above, synaptic excitation must decay sufficiently quickly for the tonic cell to jump down to the silent phase. If the decay rate becomes too slow, then both cells may in fact remain active, because the excitable cell can never escape from excitation for long enough to jump down. On the other hand, when the synaptic decay rate exceeds some level, there is little downward drift in h_t . Thus, when the excitable cell jumps down, the tonic cell remains to the right of its uncoupled homoclinic orbit and hence remains active. This leads to bursting in the excitable cell with sustained activity in the tonic cell.

The two-cell bursting solution in Fig. 12 persists from a synaptic decay rate $k=0.1$ up to at least $k=1$. However, on the upper half of that range, the tonic cell's silent phase and the excitable cell's active phase are both quite short. The two-cell bursting in Fig. 13 persists on $k \in [0.3, 0.5]$, while the tonic cell's silent phase becomes less pronounced as k is increased past 0.5. A full sensitivity analysis and exploration of the roles of synaptic and other parameters in the system, as well as the extension of this effect to larger populations of cells, remain for future work.

IV. DISCUSSION

This work demonstrates how excitatory synaptic coupling between an excitable cell and a tonically active cell can cause the two cells to burst repeatedly. Illustrations are given using the pre-BötC cell model of Butera *et al.* [15,16], but the results here apply for general single-cell models that give rise to relaxation oscillations or to square-wave bursting conditionally (i.e., when tuned appropriately) and that feature two time scales. In Sec. II C, specific conditions are given for a unique, asymptotically stable periodic bursting solution to exist in the singular limit in the conditional relaxation oscillator case, under the assumption that excitation decays on the fast time scale. The bursting solution consists of episodes when both cells are active and others when both cells are silent, with fast transitions between these episodes. The transition from the silent to the active phase is initiated by the tonic cell, while that from the active to the silent phase is led by the excitable cell. The excursion times through these phases sum to give the burst period, since the analysis is done in the singular limit. A key aspect of the bursting solution is that activity in the tonic cell can be shut off due to the enhanced decay of its slow variable that occurs in the active phase when the excitable cell is also active. Once excitation is removed, the tonic cell cannot remain active at the lowered level of its slow variable. This mechanism, through which the application of excitation can interrupt activity, is an extension of the similar mechanism presented in earlier work by Rowat and Selverston [26] and can be viewed as an active phase version of post-inhibitory rebound (e.g. Refs. [22–24]), in which the removal of hyperpolarization can induce activity.

While a specific parameter was used to introduce heterogeneity in the examples shown, any form of heterogeneity that leads to these conditions being satisfied, such as heterogeneity in the leak reversal potential [16,17,19], will lead to coupling induced bursting. Moreover, these conditions extend naturally to slower synaptic decay and to the square-wave bursting case, although in the latter, oscillations in synaptic strength in the active phase introduce subtleties for which a full treatment would necessitate a more careful analysis. As mentioned in Sec. III, there may be a range of synaptic decay rates over which the coupled cells burst in the square-wave case. This range could likely be extended to slower decay rates in the presence of some form of intrinsic adaptation or synaptic depression, which could promote the return of the recruited excitable cell to the silent phase.

For the bursting conditions derived here to be satisfied, it is important for the synaptic coupling strength to be sufficiently large. Large coupling strengths can significantly affect the location of nullclines and other bifurcation structures. In particular, because the reversal potential of synaptic excitation is closer to the voltages present in the active phase than in the silent phase, a stronger coupling is needed to enable the tonic cell to become silent than is needed to enable the excitable cell to become active. Once coupling is strong enough and the other conditions for which bursting occurs are met, the two-cell system does not exhibit bistability. In particular, once coupling is introduced, the state in which one cell is silent and the other is active is no longer a

TABLE I. Parameter values for pre-BötC cell models.

Parameter	Value	Parameter	Value	Parameter	Value	Parameter	Value
g_{NaP}	2.8 nS	E_{Na}	50.0 mV	$\theta_{m,P}$	-40 mV	$\sigma_{m,P}$	-6 mV
		$\bar{\tau}_h$	10000 ms	θ_h	-48 mV	σ_h	6 mV
g_{Na}	28 nS			θ_m	-34 mV	σ_m	-5 mV
g_K	11.2 nS	E_K	-85.0 mV				
		$\bar{\tau}_n$	10 ms	θ_n	-29 mV	σ_n	-4 mV
g_L	2.8 nS	E_L	-65.0 mV	C_m	21 pF	E_{syn-e}	0 mV
α_s	0.2 ms^{-1}	τ_s	See text	θ_s	-10.0 mV	σ_s	-5 mV

solution. A wide variety of related issues, such as coexistence of periodic bursting with other solutions away from the singular limit, the effects of heterogeneity in larger networks (see Refs. [16,19]), and variations that arise as the conditions given here break down, remain to be considered.

Finally, the results given here relate to an ongoing debate about the source of rhythmic bursting in the pre-BötC of the mammalian brainstem and the precise role of the pre-BötC in respiration [1,4–6,9,7,18,10,11,8,12]. In particular, the importance of intrinsically bursting cells in driving rhythmic bursting in the pre-BötC remains unclear. This work characterizes a mechanism that harnesses the burst-supporting persistent sodium current to generate emergent bursting in a synaptically coupled network of model pre-BötC cells, without any intrinsically bursting cells present. The existence of such a mechanism illustrates the capacity of excitatory synaptic coupling and heterogeneity to induce stable, rhythmic activity. A key next step toward understanding rhythmicity in the pre-BötC will be to consider whether analogous mechanisms arise under various combinations of pacemaker currents as well as under various levels of blockade of these currents [9,18,10–12].

ACKNOWLEDGMENTS

This work was partially supported by the National Sci-

ence Foundation Grant No. DMS-0414023. The author thanks Jeff Smith for useful discussions that motivated this work and Christopher Del Negro for a careful reading of the paper.

APPENDIX

System (19) was introduced in Refs. [15,16]. In these equations, for $x \in \{m_P, m, h, n, s\}$, the function $x_\infty(v)$ takes the form $x_\infty(v) = \{1 + \exp[(v - \theta_x)/\sigma_x]\}^{-1}$, and for $x \in \{h, n\}$, the function $\tau_x(v)$ takes the form $\tau_x(v) = \bar{\tau}_x / \cosh[(v - \theta_x)/2\sigma_x]$. The parameter values used in these equations are listed in Table I, which is also identical to that given in Ref. [20] except that there, a parameter ϵ was specifically factored out of $\bar{\tau}_h$, and here, τ_s is given in the text.

System (4) is derived from system (19) by setting $g_{Na} = g_K = 0$ and taking $-I_{tonic-e}$ to be a constant, denoted I_{app} in system (4). The value I_{app} was set at 15.4 pA for both cells in the simulations shown. A few parameters were also adjusted in simulations of system (4), namely $\theta_{m,P} = -38$ mV, $\bar{\tau}_h = 100$ ms, $\theta_s = -33$ mV, $\sigma_s = -1$ mV, and $C_m = 0.1$ pF, the last of which accentuates the relaxation aspect of the oscillations studied. Further, for system (4), I took $\tau_s = 6.25$ ms, $g_{syn} = 0.7$ nS, and introduced heterogeneity in θ_h , giving it the value -44 mV for the excitable cell and -31 mV for the tonic cell.

-
- [1] J. C. Smith, H. H. Ellengerger, K. Ballanyi, D. W. Richter, and J. L. Feldman, *Science* **254**, 726 (1991).
 - [2] S. M. Johnson, J. C. Smith, G. D. Funk, and J. L. Feldman, *J. Neurophysiol.* **72**, 2598 (1994).
 - [3] N. Koshiya and J. C. Smith, *Nature (London)* **400**, 360 (1999).
 - [4] J. C. Rekling and J. L. Feldman, *Annu. Rev. Physiol.* **60**, 385 (1998).
 - [5] J. C. Rekling, X. M. Shao, and J. L. Feldman, *J. Neurosci.* **20**, 1 (2000).
 - [6] J. C. Smith, R. J. Butera, N. Koshiya, C. DelNegro, C. G. Wilson, and S. M. Johnson, *Respir. Physiol.* **122**, 131 (2000).
 - [7] J. L. Feldman, G. S. Mitchell, and E. E. Nattie, *Annu. Rev. Neurosci.* **26**, 239 (2003).
 - [8] J. L. Feldman and C. A. DelNegro, *Nat. Rev. Neurosci.* **7**, 232 (2006).
 - [9] C. A. DelNegro, C. Morgado-Valle, and J. L. Feldman, *Neuron* **34**, 821 (2002).
 - [10] F. Peña, M. A. Parkis, A. K. Tryba, and J.-M. Ramirez, *Neuron* **43**, 105 (2004).
 - [11] C. A. DelNegro, C. Morgado-Valle, J. A. Hayes, D. D. Mackay, R. W. Pace, E. A. Crowder, and J. L. Feldman, *J. Neurosci.* **25**, 446 (2005).
 - [12] J. F. R. Paton, A. P. L. Abdala, H. Koizumi, J. C. Smith, and W. M. St-John, *Nat. Neurosci.* **9**, 311 (2006).
 - [13] J. Rinzel, "A formal classification of bursting mechanisms in excitable systems," in *Proceedings of the International Congress of Mathematicians*, edited by A. M. Gleason (American Mathematical Society, Providence, RI, 1987), pp. 1578–1594.
 - [14] E. M. Izhikevich, *Int. J. Bifurcation Chaos Appl. Sci. Eng.* **10**, 1171 (2000).

- [15] R. J. Butera, J. Rinzel, and J. C. Smith, *J. Neurophysiol.* **81**, 382 (1999).
- [16] R. J. Butera, J. Rinzel, and J. C. Smith, *J. Neurophysiol.* **81**, 398 (1999).
- [17] C. A. DelNegro, S. M. Johnson, R. J. Butera, and J. C. Smith, *J. Neurophysiol.* **86**, 59 (2001).
- [18] I. A. Rybak, N. A. Shevtsova, W. M. St-John, J. F. R. Paton, and O. Pierrefiche, *Eur. J. Neurosci.* **18**, 239 (2003).
- [19] J. Rubin and D. Terman, *SIAM J. Appl. Dyn. Syst.* **1**, 146 (2002).
- [20] J. Best, A. Borisyuk, J. Rubin, D. Terman, and M. Wechselberger, *SIAM J. Appl. Dyn. Syst.* **4**, 1107 (2005).
- [21] J. L. Feldman and J. C. Smith, *Ann. N.Y. Acad. Sci.* **563**, 114 (1989).
- [22] D. Golomb, X.-J. Wang, and J. Rinzel, *J. Neurophysiol.* **72**, 1109 (1994).
- [23] D. Terman, N. Kopell, and A. Bose, *Physica D* **117**, 241 (1998).
- [24] J. Rubin and D. Terman, "Geometric singular perturbation analysis of neuronal dynamics," in *Handbook of Dynamical Systems, Vol. 2: Towards Applications*, edited by B. Fiedler (Elsevier, Amsterdam, 2002).
- [25] D. Somers and N. Kopell, *Biol. Cybern.* **68**, 393 (1993).
- [26] P. Rowat and A. Selverston, *J. Comput. Neurosci.* **4**, 129 (1997).
- [27] P. Smolen, J. Rinzel, and A. Sherman, *Biophys. J.* **64**, 1668 (1993).
- [28] A. Sherman, *Bull. Math. Biol.* **56**, 811 (1994).
- [29] Gerda de Vries and Arthur Sherman, *Bull. Math. Biol.* **63**, 371 (2002).
- [30] G. de Vries and A. Sherman, "Beyond synchronization: modulatory and emergent effects of coupling in square-wave bursting," in *Bursting: The Genesis of Rhythm in The Nervous System*, edited by S. Coombes and P. Bressloff (World Scientific, Singapore, 2005).
- [31] E. F. Mischenko, Yu. S. Kolesov, A. Yu. Kolesov, and N. Kh. Rozov, *Asymptotic Methods in Singularly Perturbed Systems* (Plenum, New York, 1994).
- [32] J. Rubin and D. Terman, *Neural Comput.* **12**, 597 (2000).
- [33] J. Rubin and D. Terman, *J. Math. Biol.* **41**, 513 (2000).